



HAL
open science

Tropical forest structure and understorey determine subsurface flow through biopores formed by plant roots

Jérôme Nespoulous, Luis Merino-Martín, Yogan Monnier, Diane Bouchet, Merlin Ramel, Rodolphe Dombey, Gaelle Viennois, Zhun Mao, Jiao-Lin Zhang, Kun-Fang Cao, et al.

► To cite this version:

Jérôme Nespoulous, Luis Merino-Martín, Yogan Monnier, Diane Bouchet, Merlin Ramel, et al.. Tropical forest structure and understorey determine subsurface flow through biopores formed by plant roots. CATENA, 2019, 181, pp.104061. 10.1016/j.catena.2019.05.007 . hal-02149518

HAL Id: hal-02149518

<https://hal.science/hal-02149518>

Submitted on 1 Jul 2021

HAL is a multi-disciplinary open access archive for the deposit and dissemination of scientific research documents, whether they are published or not. The documents may come from teaching and research institutions in France or abroad, or from public or private research centers.

L'archive ouverte pluridisciplinaire **HAL**, est destinée au dépôt et à la diffusion de documents scientifiques de niveau recherche, publiés ou non, émanant des établissements d'enseignement et de recherche français ou étrangers, des laboratoires publics ou privés.

17 **Abstract**

18 Erosion and mass wasting processes on mountain slopes can benefit from or be adversely
19 affected by the presence of biopores formed by plant root systems or soil fauna. The relationship
20 between biopores and subsurface flow during rainstorms is poorly understood. Here, we
21 examined the link between subsurface flow and biopores formed through different processes,
22 including soil faunal activity and abundance of fine and coarse roots. As the distribution of
23 biopores is influenced by the type of vegetation present, we investigated the effect of plant
24 diversity (forest with or without understorey vegetation) on the pattern of water infiltration
25 throughout the soil. We hypothesized that increased species diversity would enhance the
26 extension of subsurface flow because biopores would be distributed throughout the soil profile
27 and that more coarse roots would create large biopores, increasing subsurface flow. *In situ*
28 experiments were conducted on hillslopes with plantations of rubber trees (*Hevea brasiliensis*)
29 growing on terraces, or with secondary mixed forests, in the tropical zone of Yunnan province,
30 China. Three sites with Ferralsol soils and different vegetation types were examined: (1)
31 plantation with no understorey; (2) clear-cut plantation with understorey; and (3) secondary
32 mixed forest with understorey. Irrigation experiments with Brilliant Blue FCF dyed water were
33 performed upslope of trees at each site and staining patterns resulting from infiltrated dyed
34 water were examined at two different scales. After dye irrigation, soil was removed in 1.0 × 0.8
35 m slices starting 1 m downslope and soil profiles were photographed for subsequent mapping of
36 dyed areas in the profile (macroscale). Each profile was then divided into a 0.1 × 0.1 m grid
37 (microscale) and burrows formed by macrofauna and fine and coarse root densities were
38 measured. At the macroscale, the greatest lateral extension in subsurface flow occurred in the
39 natural forest and the least in the rubber tree plantation with no understorey vegetation. At the
40 microscale, and in all types of vegetation, fine roots significantly increased the incidence of
41 subsurface flow compared to coarse roots and macrofauna activity. We conclude that in tropical
42 Ferralsols, fine roots, and hence understorey vegetation, play a positive role in promoting
43 subsurface flow and therefore reducing water erosion and mass wasting processes. Thus,

44 planting mixtures that include a diversity of species and strata could significantly improve soil
45 conservation.

46 **Keywords**

47 Brilliant blue, Ferralsol, *Hevea brasiliensis*, mass wasting processes, preferential flow, root
48 density mapping,

49

50 **1. Introduction**

51 Water erosion and mass wasting processes, such as shallow landslides, are recurring problems
52 around the world (Sidle and Ochiai, 2006; Stokes et al., 2013), notably in mountainous areas that
53 are particularly vulnerable to anthropogenic pressure and global change (Elkin et al., 2013). In
54 Southeast Asia, and China in particular, soil degradation on steep slopes has been accelerated
55 during the last 50 years, due to poor farming practices, deforestation, road and dam
56 construction (Sidle et al., 2006; Stokes et al., 2010; Sidle et al., 2014). The conversion of large
57 swaths of tropical rainforest to rubber tree (*Hevea brasiliensis* Mull. Arg.) plantations has also
58 led to major soil erosion and concerns about water cycling (Ziegler et al., 2009; Ahrends et al.,
59 2015; Häuser et al., 2015). In steep areas, the frequent practice of constructing bench terraces
60 before planting rubber trees changes soil physical and hydrological properties: (1) soil in the
61 bench terraces is destabilized by excavation and terrace construction (Sidle et al., 2006), and (2)
62 herbicides are used to remove understorey vegetation and the unvegetated riser faces are more
63 vulnerable to surface erosion than the original slope (van Dijk, 2002; Liu et al., 2015). Terraces
64 need constant maintenance and after forest operations such as clear-felling, they are susceptible
65 to failure because of changes in hydrological regime, such as an increase of the heterogeneity of
66 infiltration and wetting front (Fredlund et al., 2012), which correspond to vertical macropore
67 flow towards the potential slip plane (Cammeraat et al., 2005), or increases in the weight of soil
68 water (overburden effect). Therefore, to better manage soil conservation in rubber tree
69 plantations, it is necessary to understand how water moves through soil along natural and

70 terraced slopes.

71 Hydrological and mass wasting processes on vegetated slopes are influenced by soil structure
72 and plant root system morphology (Sidle and Ochiai, 2006). Water flows through two domains
73 within soils: (i) soil matrix flow, consisting of both uniform saturated and unsaturated flow
74 through fine pores and (ii) uniform and non-uniform preferential flow, occurring inside of single
75 or interconnected system of macropores with diameters >2 mm, although preferential flow can
76 also occur in more narrow pores (Tsuboyama et al., 1994; Sidle et al., 2001) and (iii) if the
77 macropores are not maintained by live roots, fauna or the frequent passage of water, they
78 gradually disappear and become “invisible pores”, or mesopores, but are still very permeable
79 and contribute significantly to preferential flow (Tsukamoto and Ohta, 1988). Biotic macropores
80 (or biopores, Figure S1) include root channels (Mitchell et al., 1995), particularly large diameter
81 (coarse) roots (Bodner et al., 2014) and faunal burrows (Noguchi et al., 1997a; Farenhorst et al.,
82 2000; Shuster et al., 2002; Weiler and Naef, 2003), while non-biotic macropores are formed by
83 freeze-thaw, wetting-drying, dissolution of soil materials, physicochemical soil aggregation, and
84 subsurface erosion (Aubertin, 1971). Root systems can create stable channels when growing in
85 the soil, largely through: (i) compression of soil particles as the root penetrates the soil and (ii)
86 amalgamation of soil particles with sloughed root cells and mucilage (Bengough et al., 1997).
87 Both live and dead plant roots can promote slope drainage by functioning as hillslope-scale
88 subsurface flow paths that drain subsurface water away from potentially unstable sites (Noguchi
89 et al., 1999, 2001). Conversely, when root channels converge or when subsurface flow abruptly
90 terminates in the slope (e.g., dead-end channels), water pressure may concentrate in critical
91 zones of the slope, thus promoting instability. Therefore, flow paths can exert both positive and
92 negative consequences on slope stability (Ghestem et al., 2011; Sidle and Bogaard, 2016). The
93 effects of different land-use types on water flows in soil have been studied with a focus on soil
94 hydraulic properties related to matrix flow (Schwartz *et al.*, 2003; Bodhinayake and Cheng Si,
95 2004; Bormann and Klaassen, 2008, Wu et al., 2017) more than preferential flow (Vogel *et al.*,
96 2006). It is not well known how different types of vegetation and land-use influence preferential

97 flow paths and especially how root morphology and pedofaunal activity affect the formation,
98 density and diameter of biopores.

99 Recently, Jiang et al., (2017, 2018) studied patterns of water infiltration through soil in rubber
100 tree plantations in Yunnan, China, using a single infiltration cylinder (with a diameter of 0.2 m).
101 Although infiltration was greater in rooted soil compared to bare soil, the effects of preferential
102 flow in biopores and matrix flow (in pores < 2mm in diameter) could not be distinguished. In
103 particular, the impact of coarse roots (> 2 mm in diameter) cannot be determined with small
104 diameter infiltration cylinders because of scaling and edge effects (Ghestem et al 2009; Zhang et
105 al 2017; Sidle et al., 2017). Coarse roots are thought to play a major, but poorly understood role,
106 in preferential flow processes (Lange et al 2009, Ghestem et al., 2011) but few field data are
107 available to quantify the effect (Wang and Zhang, 2017).

108 We explored the mechanisms through which root systems and soil macrofauna play a role on
109 subsurface flow processes along forested hillslopes in Yunnan, China. We hypothesized that: (i)
110 natural, mixed forests would have a greater extension of subsurface flow compared to
111 monospecific rubber tree plantations, because biopores should be distributed throughout the
112 entire soil profile, due to the increased diversity of insect and plant species and their different
113 root system morphologies, and (ii) a greater number of coarse roots would increase subsurface
114 flow. To understand the processes occurring, two different scales were considered: the pattern
115 of water infiltration throughout the soil profile, which reflected the impact of vegetation type on
116 subsurface flow (macroscale) and a finer 'microscale,' whereby the effects of the density and size
117 of individual roots and burrows on infiltration were elucidated.

118

119 **2. Materials and methods**

120 **2.1. Study sites**

121 Study sites were located on the Nan Lin Shan mountain of Xishuangbanna, Yunnan province,

122 China. All sites were located on slopes around Bashayicun village (21°56'31.70"N;
123 100°50'49.60"E), 10 km south of Jinghong in the Mekong catchment. The climate is tropical with
124 a mean annual temperature of 24.7°C and mean annual precipitation of 1145 mm (mean values
125 for the period 2013 – 2015 in Jinghong), with 82% of precipitation occurring during the
126 monsoon season. Slope gradient ranged from 30° to 40° and all sites were situated at an altitude
127 of about 800 m. In this region, soil surface erosion is severe and numerous landslides occur,
128 usually on farmed slopes or in rubber tree (*Hevea brasiliensis* (Willd. ex A. Juss.) Müll. Arg.)
129 plantations, during the monsoon season (May – September).

130 2.2. *Vegetation types*

131 Three sites were chosen within a landscape dominated by rubber tree plantations (Figure 1). All
132 sites were close together and similarly oriented: i) '*plantation*' corresponding to a 0.45 ha
133 rubber tree stand. Soil between tree lines was largely bare as some leaf litter was observed
134 during the autumn and herbicides were regularly used to kill herbaceous vegetation, ii) '*clear-*
135 *cut*' comprising a 0.41 ha site where rubber trees were felled in 2011. One year after this felling,
136 young rubber trees were planted as rootstock, with one plant beside each remaining tree stump.
137 Herbaceous vegetation was also present, that was colonizing the recently exposed soil (Table 1),
138 and iii) '*forest*' which consisted of mixed secondary forest without any associated crops (Figure
139 1). A diversity of tree species, shrubs, grass and litter was present at the forest site (Table 1);
140 total tree density was 11795 trees ha⁻¹ within the entire 7 ha *forest* site.

141 Rubber tree plantations (*plantation* and *clear-cut* sites) were grown on man-made terraces
142 (with a 'cut' slope about 0.8 m high and with a distance between terraces that was about 2.0 m
143 wide). Although the terraces may have different slope morphologies compared to the *forest* site,
144 and thus have altered soil structural properties, both *plantation* and *clear-cut* had the same type
145 of terraces and so were comparable. Rubber trees were planted as rootstock at an initial density
146 of 500 trees ha⁻¹. Root system morphology of these trees has not been measured, but is likely to
147 comprise a taproot with superficial, lateral roots (Masson and Monteuuis 2017). At the

148 *plantation* site, rubber trees were planted in 2006; mean diameter at breast height (DBH) was
149 15.4±0.7 cm and mean height was 11.0±4.0 cm. At the *clear-cut* site, trees were planted in 1981
150 and after felling in 2011, stumps were not removed, therefore some root decomposition may
151 have occurred belowground. The different types of vegetation meant that subsurface flow had to
152 be analysed at the microscale, with a careful analysis of root size and distribution patterns in the
153 soil.

154 We assessed vegetation composition in three 9 m² (3 × 3 m) plots spaced 4 m apart within each
155 of the three sites. In all sites, plots were located mid-slope to avoid changes in topography and
156 slope (i.e. upper and lower parts of the slope with different gradients, Figure 1c). In the
157 *plantation* and *clear-cut* sites, the centres of the plots were situated 1.5 m upslope of a tree or
158 stump of *H. brasiliensis*. At the *forest* site, plot centres were situated 1.5 m above three different
159 tree species representatives of the natural mixed forest community (*Anthocephalus chinensis*
160 (Lam.) Rich. ex Walp., *Aporosa yunnanensis* (Pax & K.Hoffm.) F. P. Metcalf and *Archidendron*
161 *monadelphum* (Roxb.) Nielson var. *monadelphum*, Table 1).

162 2.3. **Soil**

163 Soil analyses were conducted on fractions finer than 2 mm. Percentage sand (2 mm - 50µm), silt
164 (50 µm - 2 µm), and clay (<2 µm) content was determined using the pipette method (NF X31-
165 107, 2003: 31–107). The soil colour of each horizon was determined using a Munsell colour
166 chart (Munsell, 2000). Bulk density measurements were made during the analysis of soil profiles
167 (see section 2.5, Table S1, Figure S2).

168 Soil profiles were similar among sites and were classified as Ferralsols according to the FAO soil
169 classification (IUSS Working Group WRB, 2015) or laterites (oxisols) according to the Chinese
170 and USDA soil classification (Gerasimova, 2010; Soil Survey Staff, 2014). These soils were
171 developed from arenaceous shale sediments (Wang *et al.*, 1996; Cao *et al.*, 2006; Xiao *et al.*,
172 2014). Soils were described using methodology from FAO (2006) and Soil Science Division Staff
173 (2017). Soil surfaces were covered by a shallow humus layer with fast decomposition classified

174 as "mull" (Graefe et al., 2012). Soils were characterised by a litter layer (O_L) of 0.5 to 0.10 m in
175 *forests* that was absent in *clear-cut* (Figure 2). The organic decomposed horizon (O_H) was not
176 present as litter as it is quickly mineralised by faunal activity (especially termites). Soils were
177 differentiated by three characteristic soil horizons with gradual and smooth boundaries (Table
178 2, Figure 2). An A-horizon was present in the upper 0–0.3 m of soil (*surficial*), characterised by a
179 massive structure with weak to moderate thin granular to blocky peds (FAO, 2006 ; Soil Science
180 Division Staff, 2017), a clayey texture, a dark yellowish brown colour (Munsell, 2000) and the
181 presence of roots. A B-horizon existed at 0.3-0.6 m deep (*middle*) with less roots, a massive to
182 layered structure with thin blocky peds, a clayey texture and a strong brown colour. A C-horizon
183 was present in the subsoil (0.6-0.8 m - *deep*) with few roots, a massive to layered structure with
184 moderate crumbly peds, clayey texture, a reddish yellow colour and with more gravel and stones
185 at depth, depending on the occurrence of parent rock material. Throughout the profile, soils
186 were slightly moist, acidic ($\text{pH} = 4.8 \pm 0.1$) and organic matter content decreased with depth
187 from 4.6% (A-horizon) to 2.7% (B-horizon) to 1.7% (C-horizon).

188 **2.4. Dye infiltration experiments**

189 The experiments were conducted in August 2014, i.e. during the monsoon season, with a water
190 soil content close to water field capacity. The litter layer was removed and the surface soil water
191 content (0-0.1 m depth) was measured along the border of plots (as described in section 2.2),
192 before each infiltration experiment, to verify the homogeneity of surface soil moisture between
193 plots for each site. Five surface soil samples per plot were collected and soil moisture measured
194 by the gravimetric method (soils were dried for 48 hours at 105 °C (NF ISO 11465, 1994)).
195 *Plantation* plots possessed higher surface soil moisture ($49\% \pm 4\%$) than the *clear-cut* ($34\% \pm$
196 3%) and *forest* ($29\% \pm 3\%$) sites. Within each site, no significant differences in soil moisture
197 were found among plots.

198 Within each plot, we performed one dye infiltration test to visualise the effect of biopores and
199 capture the effects of root systems on flow pathways. Dye infiltration tests have been performed

200 successfully using infiltrometers and irrigation experiments (Noguchi et al., 1997b; Alaoui and
201 Goetz, 2008; Gerke et al., 2015; Clark and Zipper, 2016; Zhang et al., 2016). We prepared 60 L of
202 dye, using 480 g of Brilliant Blue FCF powder (a food dye E133 with a relatively low toxicity, low
203 sorption and high mobility (Flury and Flühler, 1994)), diluted in ordinary tap water (i.e., a
204 concentration of 4 g L⁻¹).

205 Before irrigation tests, we cut herbaceous plants with scissors at ground level and removed any
206 debris and coarse litter from the soil surface, without disturbing the soil structure. Within each
207 plot, dyed water was irrigated at a distance of 1.5 m upslope of the tree stem (Figure 3a,b). We
208 chose to apply the dye at this distance to (i) avoid direct flow of dye close and around the stem
209 bole, (ii) to avoid being too close to the upper terrace and (iii) at a distance greater than 1.5 m,
210 we may not have been able to locate blue dye downslope of the tree. Dye was stored in a tank
211 and applied by pouring it into a 1.0 m long x 0.1 m wide drainpipe perforated with 30 holes (2
212 mm in diameter). This drainpipe defined the upper limit of a 1.0 m² quadrat, which was the
213 focus of further experimental steps and analyses. Dye seeped through the pipe and into the soil
214 at a constant discharge of 10.0 ml s⁻¹ (Roose, 1980; Asseline et al., 1993). Discharge was kept
215 relatively constant by keeping water at the same level in the pipe during each test. To promote
216 infiltration, surface runoff was blocked by a metal sheet dam (1.0 m long by 0.08 m deep) 0.3 m
217 downslope of the drainpipe (Figure 3a,b).

218 2.5. *Soil profile analysis*

219 After 5 hours of infiltration, the soil profile was excavated to bedrock (to a maximum depth of
220 0.8 m). Soil was carefully removed to produce a smooth profile wall surface, starting from the
221 lower limit of the plot (1.0 m downslope of the irrigation source). A new profile was then made
222 0.1 m uphill and repeated until 10 soil profiles were excavated. We termed the analysis of these
223 profiles as the “macroscale analysis” that captured the effects of vegetation type on the
224 extension of subsurface flow. To investigate the effects of insect burrows and root size and
225 density on infiltration at the microscale, a 1.0 x 0.8 m grid divided into 0.1 m squares was set in

226 front of each profile (Figure 4a). Profiles were then photographed to show the intensity and
227 distribution of blue dye for mapping and recording results. Photographs were taken using a
228 digital camera (Nikon D7000 – Lens 18-105 f/3.5-5.6: 1/125 seconds; 5.6 obturator; ISO 200;
229 WB 5500K) situated 1.0 m from each profile on a tripod focused on the centre of the profile. We
230 used a flash (Yongnuo 560II), projected at 45° on a reflector located 1.0 m above the profile and
231 parallel to the slope, to mitigate the brightness differences related to sunshine cycles and forest
232 cover. A neutral grey scale was used to fill and reduce the variability of colour on each
233 photograph.

234 After each irrigation test, three vertical soil profiles were selected for further analysis: the
235 furthest profile from the drainpipe, where dye was present (thus representing the longest
236 subsurface flow path), and two other profiles, situated at equal distances between the furthest
237 profile with blue dye present and the drainpipe. In these three profiles we measured the root
238 diameter with a calliper and we classed roots into two diameter classes: fine (≤ 2 mm) and
239 coarse (> 2 mm). In each square, we counted the number of roots present in each class. We
240 distinguished decayed (roots were dark in colour and broke easily) *versus* not decayed and dyed
241 *versus* not dyed roots. The presence of biopores generated by soil macrofauna (e.g., termites,
242 ants and worms) such as galleries, cavities, and loosened soil in each cell were visually identified
243 (supplementary material Figure S1). In these three soil profiles, we also collected two soil
244 samples from horizons A and B with a sealed cylinder corer (100 cm³) to measure bulk density
245 (NF X31-501, 1992). A manual sampling of 50 to 100 g of soil was carried out at the same
246 locations and with the addition of the possibility of sampling in horizon C to measure soil water
247 content (supplementary material Figure S3, Tables S2, S3). Samples were weighed at field
248 moisture content and then dried in the laboratory for 48 hours in an oven at 105°C and re-
249 weighed (NF ISO 11465, 1994). No significant differences among plots occurred within sites and
250 a general decrease of soil water content with depth was found (supplementary material Figure
251 S3, Table S3).

252 To examine if soil resistance to penetration, and hence compaction, affected subsurface flow, we

253 measured soil resistance using a penetrometer (Humboldt, Dial Pocket Penetrometer H-4205,
254 plunger diameter = 5 mm) in the four corners of each of the 0.1 m squares of the profile. When
255 possible, an additional measurement was added in and at the side of the stained area. From
256 these data we calculated the average penetration resistance per square Soil resistance to
257 penetration is generally affected by soil water content. As we did not find significant differences
258 in soil water patterns among plots within sites (Figure S3, Table S3), the comparisons of soil
259 resistance to penetration were considered as valid.

260 2.6. *Image analysis*

261 The surface area of stained regions was determined from photographs for each selected soil
262 profile. Several steps were necessary in order to obtain data that could quantify the coloured
263 area specifically in relation to depth and intensity of blue colour (Figure 4). First, we
264 recalibrated colours and luminosity with respect to the neutral grey scale placed on the profile
265 while taking photographs and by de-skewing colour histograms using the Lightroom 6.0
266 software (Adobe developer team, 2016, Figure 4a). Then, the saturation of the blue stains was
267 maximised to facilitate the differentiation of the dyed intensity. Thus, two main contrasting
268 colours were obtained: green corresponding to blue and grey corresponding to soil (Figure 4b).
269 We then used the geographic information system program QGIS 2.16 (QGIS Development Team,
270 2016) to de-skew orthogonally and spatialize the pictures by georeferencing (Geodesic System
271 WGS84; Transverse Universelle the Mercator 31T; polynomial 3 points, nearest neighbours).
272 Finally, we classified colour by using the eCognition 9.0.3 software (eCognition developer team,
273 2016) 'object classification' mode (GIS complementary software) to obtain two classes: 'soil' and
274 'blue' (Figure 4c). The shapefile generated by eCognition was imported into Qgis to dissolve
275 polygons by colour classes and intersect them with a referenced spatialised grid to obtain a
276 shapefile with data of area colour classes for each 0.1 m square within a profile. With these data,
277 we could calculate the surface area stained within each 0.1 x 0.1 m square. We did not analyse
278 specific dimensions related to the shape of the stained areas.

279 2.7. *Data analysis*

280 We analysed data at two scales: i) at the macroscale (1.0 x 0.8 m) to describe how different
281 vegetation types influenced the lateral extension of subsurface flow and ii) at the microscale (in
282 squares of 0.1 x 0.1 m) to describe how the presence of root and insect burrows affect water
283 flow distribution.

284 At the macroscale, the number of roots per diameter class (< and > 2 mm diameter classes), the
285 presence of fauna, and resistance to penetration were aggregated at three soil depths for each
286 test. These depths corresponded to '*surficial*' (0-0.3 m), which included O and A horizons,
287 '*middle*' (0.3-0.6 m) comprising the B horizon, and '*deep*' (0.6-0.8 m) corresponding to the C
288 horizon. Soil profile depths were different among sites, so the C horizon was not always reached.
289 For the *forest* and *plantation* sites, the C horizon was only present at one and two sites,
290 respectively (Figure 2). The influence of vegetation type and depth on roots and insect burrows,
291 and resistance to penetration were investigated using Kruskal Wallis and Wilcoxon tests to
292 specify pairwise differences, as data did not follow a normal distribution.

293 At the microscale, each 0.1 x 0.1 m square was considered a sample. Data from above and below
294 the dam were analysed separately because they were linked to different hydrological processes.
295 Generally, flow was considered 'matrix flow' when a homogeneous wetting front was observed,
296 whilst 'preferential flow' was when isolated blue dye patches and wetting front instabilities
297 were observed (Cammeraat et al., 2005; Fredlund et al., 2012). We investigated if the subsurface
298 dye distribution was affected by the following factors: (i) depth (in 0.1 m classes from 0 to 0.8
299 m), (ii) downslope distance from the dye source, (iii) fine and coarse root abundance, and (iv)
300 abundance of faunal burrows. Linear models with mixed effects (LME) were used to identify
301 factors influencing the abundance of the dyed area. As fixed effects, we tested different
302 combinations of factors (fine roots, coarse roots, fauna presence, soil penetration resistance and
303 depth). Plots and soil profiles were considered as random effects and the soil profiles were
304 nested inside the plots. We then selected models with different combinations of the fixed effect
305 predictors by comparing their Akaike Information Criterion (AIC, Burnham & Anderson 2002)

306 with analysis of variance (ANOVA). At the microscale, we excluded unstained areas from the
307 statistical analysis, because the absence of dye in a cell does not necessarily indicate that the
308 conditions leading to preferential flow are absent, but could be due to different reasons, such as
309 lack of dye to the cell or other preferential flows occurring prior to arrival of dye in the cell.
310 Uniquely focusing on soil cells with the presence of dye (i.e., presence of flow) enables us to
311 ascertain the relationship between roots and insect burrows and dye distribution without noise
312 in the data. Dyed areas detected by the image analyses with a surface area smaller than 0.25 cm²
313 were considered as not dyed because they were potentially artefacts related to
314 microtopography, for example microshadows. Statistical analyses were performed using R 3.3.1
315 (R Core Team, 2016) with the package 'lme4' (Bates et al. 2015) for linear models with mixed
316 effects (LME).

317 **3. Results**

318 **3.1. Subsurface flow downslope along the plot and through the profile**

319 A network of biopores comprising channels formed by roots, termites, ants and earthworms was
320 visible at every site throughout each soil profile (Figure S1). Preferential and matrix flows were
321 distinguished by examining the photographs taken for each soil profile. Above the dam, we
322 observed both homogenous matrix and preferential flows, whilst below the dam we observed
323 preferential flow only, identified as isolated blue patches (Figure 3). Preferential flow often
324 occurred in a zig-zag pattern along a distance of up to 0.9 m in the downslope direction.
325 Subsurface flows of dye travelled different distances with depth and along the slope (Figure 5).
326 The maximum horizontal extension of dyed areas differed among sites: flow in *plantation*
327 extended to a mean of 0.50 ± 0.10 m. Flow in *clear cut* extended to a mean of 0.53 ± 0.09 m and
328 in *forest*, flow was found at a mean distance of 0.67 ± 0.15 m. However, the peak of dyed areas
329 (i.e., the profile where the number of cells with the presence of blue dye was greatest) always
330 existed at a distance of 0.10-0.20 m from the dye source, at all sites.

331 3.2. *Effect of vegetation type on biopores*

332 At the macroscale, the *forest* site had a significantly greater number (42 ± 5) of coarse roots in
333 the upper 0.3 m of soil, compared to the lower soil depth classes, which were not significantly
334 different from one another (Figure 6a, $\chi^2 = 4.87$, $P = 0.08$). In the *plantation*, the number of
335 coarse roots (>2 mm) was also highest in the uppermost soil layer (11 ± 2) and decreased
336 significantly with depth (Figure 6a, $\chi^2 = 4.61$, $P = 0.10$). No significant differences were found in
337 coarse root number with any soil depth class at the *clear-cut* site (Figure 6). Due to the high
338 number of roots in the surficial soil layer at the *forest* site, the mean total number of roots over
339 the entire soil profile was significantly greater than at the *clear-cut* site, but not in the *plantation*
340 (Figure 6a, $\chi^2 = 6.93$, $P = 0.03$).

341 At all sites, the number of fine roots (<2 mm in diameter) was significantly higher in the
342 uppermost soil layer (Figure 6b, *Plantation*: 503 ± 44 , $\chi^2 = 6.25$, $P = 0.04$; *Clear-cut*: 1261 ± 163 ,
343 $\chi^2 = 7.20$, $P = 0.02$; *Forest*: 918 ± 130 , $\chi^2 = 5.14$, $P = 0.07$). The *clear-cut* site with many
344 herbaceous species present, had the greatest number of fine roots in the uppermost soil layer
345 and root numbers decreased significantly with soil depth (Figure 6b, $\chi^2 = 6.48$, $P = 0.04$). The
346 total mean density of roots in the *forest* site (1292 ± 401 roots m^{-2}) was not significantly greater
347 than in the *plantation* (871 ± 212 roots m^{-2}) or *clear-cut* (1572 ± 566 roots m^{-2}) sites, whereas
348 the latter two sites were significantly different (Figure 6b, $\chi^2 = 6.49$, $P = 0.04$). With regard to
349 biopores created by macrofauna, no significant differences in the number of biopores were
350 found among soil layers or sites (Figure 6c).

351 Soil resistance to penetration ranged from 0 to 12 kPa and increased with increasing depth in
352 the *forest* and *plantation* sites, with the greatest resistance (12 kPa) found in the deepest soil
353 layers of the *forest* site (Figure 6d, $\chi^2 = 5.14$, $P = 0.07$, compared to the surficial layer (8.4 ± 0.5
354 kPa) of the *forest* site). Therefore, mean soil resistance over the entire soil profile for the *forest*
355 site was significantly higher (11.1 ± 2.0 kPa) than for the *plantation* site (6.5 ± 1.1 kPa), even
356 though this measurement was also influenced by differences in soil moisture, but not the *clear-*
357 *cut* site (6.1 ± 0.5 kPa, Figure 6d, $\chi^2 = 5.95$, $p=0.05$). No significant differences were found

358 among soil depth classes at the *clear-cut* site.

359 Bulk density was not significantly different between sites, and for the A horizon was 0.92 ± 0.07
360 for *plantation*, 1.01 ± 0.08 for *clear-cut*, and 1.06 ± 0.1 for *forest* sites (Table 2). The B horizons
361 were more dense with values ranging from 1.09 ± 0.09 for *plantation* and 1.09 ± 0.11 for *clear-*
362 *cut* to 1.22 ± 0.09 for *forest*. The deeper horizons were dense and compact but could not be
363 sampled due to their hardness and the high rate of coarse elements (e.g., gravel, pebbles and
364 stones). The variability in bulk density was due mainly to the heterogeneity of the soil structure
365 and affected by the passage of fauna with more or less loose areas between sites (supplementary
366 material Figure S2, Table S1).

367

368 **3.3. Relationships between subsurface flow and biotic factors at the microscale**

369 At the microscale, no significant relationships between the surface area of soil stained with blue
370 dye and number of coarse roots or fauna activity were found either above or below the dam
371 (Figure S4). Based on LME for dyed cells, above the dam (i.e., matrix and preferential flows), the
372 best fitting model was that including fine root abundance in interaction with site (AIC = 3643, Df
373 = 7, Table 3, Figure S4). However, below the dam (i.e., preferential flow), the best model included
374 only the abundance of fine roots in interaction with depth (AIC = 1478, Df = 7, Table 3, Figure
375 S4). Therefore, fine roots were the most important factor affecting dyed areas when compared
376 to coarse roots or faunal channels. At each site, the importance of the presence of fine roots on
377 the dyed area, both above and below the dam, was highlighted when the total dyed area was
378 plotted as a function of fine root presence (Yes vs. No; Figs. 7a, b). For each site, a significant
379 positive linear relationship was found between fine root abundance and dyed surface area above
380 the dam, although variability in data was high (Figure 7c). The increment of dyed area due to
381 increasing fine root density was greatest at the *plantation* site (Figure 7c, Table 3: estimate =
382 2.77^{***}), intermediate at the *forest* site (Figure 7c, Table 3: estimate = 2.08^{***}) and smallest at
383 the *clear-cut* site (Figure 7c, Table 3: estimate = 1.31^{***}). For the data below the dam, the best

384 model included fine roots and interaction with depth (Figure 6d, Table 3: estimate = 0.99***).

385 **4. Discussion**

386 Subsurface flow and root distribution decreased with depth and distance from source under all
387 types of vegetation. Contrary to our hypothesis, and in all types of vegetation, these results were
388 consistent in terms of the dominant role of fine roots channelling water. We also observed
389 differences among sites for both the maximum downslope extension of dyed water flow and the
390 relationship between the dyed area and fine roots. These combined findings highlight the
391 complexity of hydrological processes in soils, at even a local scale.

392 Each site possessed its own particularities in terms of soil compaction and biotic activities,
393 resulting in disparities of subsurface flow. We found that natural forest had greater downslope
394 subsurface flow propagation than rubber tree plantations, similar to findings from Neris et al.,
395 (2012) studying natural evergreen forest and pine (*Pinus canariensis*) plantations and Marín-
396 Castro et al (2017) investigating secondary tropical montane cloud forest and coffee (*Coffea*
397 *arabica*) plantations. Bodhinayake and Si (2004) also showed that greater preferential flow
398 occurred in flat grasslands compare to cultivated soils. Other authors demonstrated higher
399 preferential flows on sites with trees than in grasslands (Joffre and Rambal, 1988; Belsky et al.,
400 1993; van Schaik, 2009; Perkins et al., 2012) or beneath trees in agroforests (Wang and Zhang
401 2017). In agreement with Zhu et al. (2018), we show that converting natural forest to
402 plantations may induce an increase of runoff due to a decrease of infiltration and subsurface
403 flow. This impact would be significantly reduced if monocropped plantations were converted to
404 e.g., alley cropping (Sun et al. 2018).

405

406 We showed that coarse root abundance was significantly greater in the upper 0.3 m of soil in the
407 *forest* site, compared to soil (shallow or deep) of any site, probably due to the greater diversity
408 and density of trees along the slope. Increasing species diversity will lead to a greater number of

409 root system morphologies and hence a more enhanced spatial occupation of the soil profile
410 (Stokes et al., 2009). Although we did not measure litter properties, enhanced litter thickness in
411 natural forests also increases hydraulic conductivity compared to plantation forests (Marín-
412 Castro et al., 2017). The greatest abundance of fine roots (<2 mm in diameter) was near the soil
413 surface in the *clear-cut* site, with many herbaceous species present, resulting in a higher
414 subsurface flow propagation in the top 0.3 m of soil, as also found by Bodhinayake and Si (2004).
415 With regard to biopores created by soil fauna, surprisingly, we did not see significant differences
416 among soil layers and sites. Léonard and Rajot, (2001) also discussed the difficulty in
417 quantifying the effect of termites on runoff and infiltration because data were highly variable.
418 These authors found a significant effect of fauna that increased infiltration and reduced runoff
419 (also shown by Beven and Germann, 1982; Yvan et al., 2012; Cheng et al., 2017; Schneider et al.,
420 2018), and Jouquet et al., (2012) showed that macrofaunal activity reduced soil erosion on a
421 fallow slope in Vietnam. Soil resistance to penetration increased with depth in *forest* and
422 *plantation* sites, with the greatest resistance found in the deepest soil layers of the *forest* site.
423 *Forest* had different soil physical properties than those of the *plantation* sites (in which the soil
424 structure was possibly affected by terrace construction). The changes in slope geometry in
425 terraced terrain can affect subsurface flow and alter the position of the wetting front
426 (Cammeraat et al., 2005; Sidle et al., 2006).

427 We highlighted the positive effect of biological activity on subsurface flow. For each of the three
428 sites, we demonstrated that live, fine roots had a more dominant effect on subsurface flow
429 compared to coarse roots and soil fauna, contrary to our initial hypothesis. This finding shows
430 the importance of considering the multiple roles of fine roots when studying the soil-plant-water
431 continuum. Fine roots, which grow fast and are usually more numerous than thicker roots, may
432 make, in a short time, many non-capillary channels that can greatly improve the soil infiltration
433 capacity. Also, fine roots should be more susceptible to soil dryness and thus more prone to root
434 shrinkage that create gaps between the root and the soil (De Roo, 1968). Fine roots also have a
435 very fast turnover rate (30 to 1000 days) and thus form dead root channels more quickly than

436 coarse roots which remain longer in the soil (McCormack and Guo, 2014; McCormack *et al.*,
437 2015; Germon *et al.*, 2016). These processes are also beneficial for enhancing soil infiltration
438 capacity.

439 Although we demonstrated that although the potential effect of land-use changes on preferential
440 flow was related to variations in the density and size of biopores, our field sites were not
441 replicated at the forest or watershed scale, therefore, it is difficult to extrapolate results beyond
442 the scale of individual trees. To understand infiltration and subsurface flow processes at a
443 greater scale, it would be necessary to perform more numerous and simpler infiltration tests, or
444 larger-scale assessments of infiltration. Nevertheless, our study contributes to the increasing
445 number of studies showing that subsurface flow and especially preferential flow, increase water
446 drainage, thereby reducing surficial runoff and erosion processes. Preferential flow can also
447 reduce the build-up of pore water pressure within soil, and so decrease the triggering of rainfall
448 induced landslides (but adverse effects are also possible, see Ghestem *et al.*, 2011). Therefore,
449 our results suggest that mixtures of species should protect against soil erosion and possibly
450 slope instability. In cultivated soils, tree and shrubby/herbaceous mixtures, such as alley
451 cropping (Jiang *et al.*, 2017), or no- or soft-intercropping weeding (Liu *et al.*, 2019), would be
452 beneficial for soil conservation.

453 **5. Conclusion**

454 We studied subsurface flow processes at the microscale (corresponding to individual biopores,
455 roots and fauna) and the macro-scale (corresponding to the soil profile around individual trees).
456 Our results show the complexity of the drivers of preferential flow in soils. The role of fine roots
457 promoting subsurface flow was dominant over macrofaunal burrows and coarse roots. The
458 consistent positive relationship between fine root density and subsurface flow can help to
459 support assumptions of the effects of roots on rapid drainage during an intense rain event. This
460 drainage should efficiently reduce surface runoff and surface erosion during heavy rainfall and
461 promote downslope drainage, which can have beneficial or adverse effects on slope stability.

462 These results demonstrate the need to consider using species mixtures in local forest conversion
463 programs to avoid mass wasting processes and soil erosion, e.g. agroforestry, alley-cropping
464 systems or plantations with understorey species present.

465 **Acknowledgements**

466 Funding was jointed provided by the BMU (Germany) International Climate Initiative funded
467 project 'Ecosystems Protecting Infrastructure and Communities' (EPIC), a French – Chinese
468 Xuguangqi program named "IMMORTEL" (Interactions between bioMechanical and
469 MORphological Root Traits and their impact on soil Erosion and Landslide mitigation, ref.:
470 34442WB) and an INRA PhD demi-bursary (JN). Thanks are due to XTBG, Eric Leveque and
471 villagers for logistic help. We are grateful to, Gilles Le Moguedec (INRA France), Pierre Honoré
472 (Photographer), Kyle Tomlinson (CAS, China), Yan Wang (CAS, China), and Don Picker (IASHK,
473 Hong Kong) for help with data analysis, soil photographic protocol management and species'
474 identification.

References

- Adobe developer team, 2016. Adobe Photoshop Lightroom. Adobe System Incorporated.
- Ahrends, A., Hollingsworth, P.M., Ziegler, A.D., Fox, J.M., Chen, H., Su, Y., Xu, J., 2015. Current trends of rubber plantation expansion may threaten biodiversity and livelihoods. *Global Environmental Change* 34, 48–58.
- Alaoui, A., 2006. Estimation du flux dans la zone non saturée. Méthode simple - Connaissance de l'environnement. Office fédéral de l'environnement (OFEV) (UW-0702-F) 52.
- Alaoui, A., Goetz, B., 2008. Dye tracer and infiltration experiments to investigate macropore flow. *Geoderma, Antarctic Soils and Soil Forming Processes in a Changing Environment* 144 (1-2), 279–286.
- Anderson, A.E., Weiler, M., Alila, Y., Hudson, R.O., 2009. Dye staining and excavation of a lateral preferential flow network. *Hydrol. Earth Syst. Sci.* 13 (6), 935–944.
- Asseline, J., De Noni, G., Nouvelot, J.-F., Roose, E., 1993. Note sur la conception et l'utilisation d'un simulateur de ruissellement. *Cahiers ORSTOM.Série Pédologie* 28 (2), 405–411.
- Aubertin, G., 1971. Nature and extent of macropores in forest soils and their influence on subsurface water movement. USDA Forest Service, Research Paper NE-192, 33.
- Bates, D., Mächler, M., Bolker, B., Walker, S., 2015. Fitting Linear Mixed-Effects Models Using lme4. *Journal of Statistical Software* 67.
- Belsky, A.J., Mwonga, S.M., Amundson, R.G., Duxbury, J.M., Ali, A.R., 1993. Comparative Effects of Isolated Trees on Their Undercanopy Environments in High- and Low-Rainfall Savannas. *The Journal of Applied Ecology* 30 (1), 143.
- Benegas, L., Ilstedt, U., Roupsard, O., Jones, J., Malmer, A., 2014. Effects of trees on infiltrability and preferential flow in two contrasting agroecosystems in Central America. *Agriculture, Ecosystems & Environment* 183, 185–196.
- Bengough, A.G., Croser, C., Pritchard, J., 1997. A biophysical analysis of root growth under mechanical stress. *Plant and Soil* 189 (1), 155–164.
- Bodhinayake, W., Cheng Si, B., 2004. Near-saturated surface soil hydraulic properties under different land uses in the St Denis National Wildlife Area, Saskatchewan, Canada. *Hydrol. Process.* 18 (15), 2835–2850.
- Bodner, G., Leitner, D., Kaul, H.-P., 2014. Coarse and fine root plants affect pore size distributions differently. *Plant Soil*, 1–19.
- Bormann, H., Klaassen, K., 2008. Seasonal and land use dependent variability of soil hydraulic and soil hydrological properties of two Northern German soils. *Geoderma, Modelling Pedogenesis* 145 (3–4), 295–302.
- Burnham, K.P., Anderson, D.R., 2002. Model selection and multimodel inference: a practical information-theoretic approach, 2nd ed. Springer.
- Cammeraat, E., van Beek, R., Kooijman, A., 2005. Vegetation succession and its consequences for slope stability in SE Spain. *Plant and Soil* 278 (1), 135–147.
- Cao, M., Zou, X., Warren, M., Zhu, H., 2006. Tropical Forests of Xishuangbanna, China. *Biotropica* 38 (3), 306–309.

- Carey, J., 2011. Storm warnings: extreme weather is a product of climate change. *Scientific American*, a Division of Springer Nature America, Inc. 128.
- Cheng, Y., Ogden, F.L., Zhu, J., 2017. Earthworms and tree roots: A model study of the effect of preferential flow paths on runoff generation and groundwater recharge in steep, saprolitic, tropical lowland catchments. *Water Resources Research* 53, 5400–5419.
- Clark, E.V., Zipper, C.E., 2016. Vegetation influences near-surface hydrological characteristics on a surface coal mine in eastern USA. *CATENA* 139, 241–249.
- DeRoo, H.C., 1968. Tillage and root growth, in: W. J. Whittington (Ed.) *Root Growth*. Butterworths. London, pp. 339–358.
- eCognition developer team, 2016. eCognition. Trimble.
- Elkin, C., Gutiérrez, A.G., Leuzinger, S., Manusch, C., Temperli, C., Rasche, L., Bugmann, H., 2013. A 2 °C warmer world is not safe for ecosystem services in the European Alps. *Glob Change Biol* 19 (6), 1827–1840.
- FAO, 2006. *Guidelines for soil description*, 4th ed. Rome.
- Farenhorst, A., Topp, E., Bowman, B.T., Tomlin, A.D., 2000. Earthworm burrowing and feeding activity and the potential for atrazine transport by preferential flow. *Soil Biology and Biochemistry* 32 (4), 479–488.
- Fattet, M., Fu, Y., Ghestem, M., Ma, W., Foulonneau, M., Nespoulous, J., Le Bissonnais, Y., Stokes, A., 2011. Effects of vegetation type on soil resistance to erosion: Relationship between aggregate stability and shear strength. *CATENA* 87 (1), 60–69.
- Flury, M., Flühler, H., 1994. Brilliant Blue FCF as a dye tracer for solute transport studies - A toxicological overview. *Journal of Environmental Quality* 23 (5).
- Fredlund, D.G., Rahardjo, H., Fredlund, M.D., 2012. *Unsaturated Soil Mechanics in Engineering Practice: Fredlund/Unsaturated Soil Mechanics*. John Wiley & Sons, Inc., Hoboken, NJ, USA.
- Gerasimova, M.I., 2010. Chinese soil taxonomy: Between the American and the international classification systems. *Eurasian Soil Sc.* 43 (8), 945–949.
- Gerke, K.M., Sidle, R.C., Mallants, D., 2015. Preferential flow mechanisms identified from staining experiments in forested hillslopes. *Hydrological Processes* 29, 4562–4578.
- Germon, A., Cardinael, R., Prieto, I., Mao, Z., Kim, J., Stokes, A., Dupraz, C., Laclau, J.-P., Jourdan, C., 2015. Unexpected phenology and lifespan of shallow and deep fine roots of walnut trees grown in a silvoarable Mediterranean agroforestry system. *Plant and Soil* 401 (1–2), 409–426.
- Ghestem, M., Sidle, R.C., Stokes, A., 2011. The influence of plant root systems on subsurface flow: implications for slope stability. *BioScience* 61 (11), 869–879.
- Graefe, U., Baritz, R., Broll, G., Kolb, E., Milbert, G., Wachendorf, C., 2012. Adapting humus form classification to WRB principles.
- Häuser, I., Martin, K., Germer, J., He, P., Blagodatsky, S., Liu, H., Krauß, M., Rajaona, A., Min, S., Pelz, S., Langenberger, G., Zhu, C.-D., Cotter, M., Stuerz, S., Waibel, H., Steinmetz, H., Wieprecht, S., Frör, O., Ahlheim, M., Cadisch, G., 2015. Environmental and socio-economic impacts of rubber cultivation in the Mekong region: Challenges for sustainable land use. *CAB Reviews*:

- Perspectives in Agriculture, Veterinary Science, Nutrition and Natural Resources 10 (27), 1-11.
- IUSS Working Group WRB, 2015. World Reference Base for Soil Resources 2014, update 2015 International soil classification system for naming soils and creating legends for soil maps, World Soil Resources Reports. No. 106. FAO, Rome.
- Jiang, X.J., Liu, W., Chen, C., Liu, J., Yuan, Z.-Q., Jin, B., Yu, X., 2018. Effects of three morphometric features of roots on soil water flow behavior in three sites in China. *Geoderma* 320, 161–171.
- Jiang, X.J., Liu, W., Wu, J., Wang, P., Liu, C., Yuan, Z.-Q., 2017. Land Degradation Controlled and Mitigated by Rubber-based Agroforestry Systems through Optimizing Soil Physical Conditions and Water Supply Mechanisms: A Case Study in Xishuangbanna, China. *Land Degradation & Development* 28, 2277–2289.
- Joffre, R., Rambal, S., 1988. Soil water improvement by trees in the rangelands of southern Spain. *Acta oecologica. Oecologia plantarum* 9 (4), 405–422.
- Jouquet, P., Janeau, J.-L., Pisano, A., Sy, H.T., Orange, D., Minh, L.T.N., Valentin, C., 2012. Influence of earthworms and termites on runoff and erosion in a tropical steep slope fallow in Vietnam: A rainfall simulation experiment. *Applied Soil Ecology* 61, 161–168.
- Lange, B., Lüscher, P., Germann, P.F., 2009. Significance of tree roots for preferential infiltration in stagnic soils. *Hydrology and Earth System Sciences* 13, 1809–1821.
- Léonard, J., Rajot, J.L., 2001. Influence of termites on runoff and infiltration: quantification and analysis. *Geoderma* 104, 17–40.
- Liu, H., Yang, X., Blagodatsky, S., Marohn, C., Liu, F., Xu, J., Cadisch, G., 2019. Modelling weed management strategies to control erosion in rubber plantations. *CATENA* 172, 345–355.
- Marín-Castro, B.E., Geissert, D., Negrete-Yankelevich, S., Gómez-Tagle Chávez, A., 2016. Spatial distribution of hydraulic conductivity in soils of secondary tropical montane cloud forests and shade coffee agroecosystems. *Geoderma* 283, 57–67.
- Liu, W., Luo, Q., Li, J., Wang, P., Lu, H., Liu, Wenyao, Li, H., 2015. The effects of conversion of tropical rainforest to rubber plantation on splash erosion in Xishuangbanna, SW China. *Hydrology Research* 46 (1), 168.
- Marín-Castro, B.E., Negrete-Yankelevich, S., Geissert, D., 2017. Litter thickness, but not root biomass, explains the average and spatial structure of soil hydraulic conductivity in secondary forests and coffee agroecosystems in Veracruz, Mexico. *Science of The Total Environment* 607–608, 1357–1366.
- Masson A., Monteouis O., 2017. Rubber tree clonal plantations: grafted vs self-rooted plant material. *Bois et Forêts des Tropiques* 332, 57-68.
- McCormack, M.L., Dickie, I.A., Eissenstat, D.M., Fahey, T.J., Fernandez, C.W., Guo, D., Helmisaari, H.-S., Hobbie, E.A., Iversen, C.M., Jackson, R.B., Leppälammil-Kujansuu, J., Norby, R.J., Phillips, R.P., Pregitzer, K.S., Pritchard, S.G., Rewald, B., Zadworny, M., 2015. Redefining fine roots improves understanding of below-ground contributions to terrestrial biosphere processes. *New Phytol* 207 (3), 505–518.
- McCormack, M.L., Guo, D., 2014. Impacts of environmental factors on fine root lifespan. *Front Plant Sci* 5.
- Mitchell, A.R., Ellsworth, T.R., Meek, B.D., 1995. Effect of root systems on preferential flow in swelling soil. *Communications in Soil Science and Plant Analysis* 26 (15–16), 2655–2666.

- Munsell Color Company, 2000. Munsell soil color charts: year 2000 revised washable edition. Neris, J., Jiménez, C., Fuentes, J., Morillas, G., Tejedor, M., 2012. Vegetation and land-use effects on soil properties and water infiltration of Andisols in Tenerife (Canary Islands, Spain). *CATENA* 98, 55–62.
- NF ISO 11465, 1994. Qualité du sol - Détermination de la teneur pondérale en matière sèche et en eau - Méthode gravimétrique. Afnor. Paris.
- NF X31-107, 2003. Qualité du sol - Détermination de la distribution granulométrique des particules du sol - Méthode à la pipette. Afnor. Paris.
- NF X31-501, 1992. Qualité des sols - Méthodes physiques - Mesure de la masse volumique apparente d'un échantillon de sol non remanié - Méthode du cylindre. Afnor. Paris.
- Noguchi, S., Rahim Nik, A., Kasran, B., Tani, M., Sammori, T., Morisada, K., 1997a. Soil physical properties and preferential flow pathways in tropical rain forest, Bukit Tarek, Peninsular Malaysia. *Journal of Forest Research* 2 (2), 115–120.
- Noguchi, S., Tsuboyama, Y., Sidle, R.C., Hosoda, I., 1997b. Spatially distributed morphological characteristics of macropores in forest soils of Hitachi Ohta Experimental Watershed, Japan. *Journal of Forest Research* 2 (4), 207–215.
- Noguchi, S., Tsuboyama, Y., Sidle, R.C., Hosoda, I., 2001. Subsurface runoff characteristics from a forest hillslope soil profile including macropores, Hitachi Ohta, Japan. *Hydrol. Process.* 15 (11), 2131–2149.
- Noguchi, S., Tsuboyama, Y., Sidle, R.C., Hosoda, I., 1999. Morphological Characteristics of Macropores and the Distribution of Preferential Flow Pathways in a Forested Slope Segment. *Soil Sciences Society of America Journal* 63 (5), 1413–1423.
- Perkins, K.S., Nimmo, J.R., Medeiros, A.C., 2012. Effects of native forest restoration on soil hydraulic properties, Auwahi, Maui, Hawaiian Islands. *Geophysical Research Letters* 39 (L05405).
- QGIS Development Team, 2016. QGIS Geographic Information System. Open Source Geospatial Foundation Project.
- R Core Team, 2016. R: A Language and Environment for Statistical Computing. R Foundation for Statistical Computing, Vienna, Austria.
- Roose, E., 1980. Dynamique actuelle d'un sol ferrallitique sablo-argileux très désaturé sous cultures et sous forêt dense humide sub-équatoriale du Sud de la Côte d'Ivoire : Adiopodoumé 1964-1975 (No. 86). ORSTOM, Paris, France.
- Schneider, A.-K., Hohenbrink, T.L., Reck, A., Zangerlé, A., Schröder, B., Zehe, E., van Schaik, L., 2018. Variability of earthworm-induced biopores and their hydrological effectiveness in space and time. *Pedobiologia* 71, 8–19.
- Schwartz, R.C., Evett, S.R., Unger, P.W., 2003. Soil hydraulic properties of cropland compared with reestablished and native grassland. *Geoderma, Quantifying agricultural management effects on soil properties and processes* 116 (1-2), 47–60.
- Shuster, W., Subler, S., McCoy, E., 2002. The influence of earthworm community structure on the distribution and movement of solutes in a chisel-tilled soil. *Applied Soil Ecology* 21 (2), 159–167.

- Sidle, R.C., Gomi, T., Loaiza Usuga, J.C., Jarihani, B., 2017. Hydrogeomorphic processes and scaling issues in the continuum from soil pedons to catchments. *Earth-Science Reviews* 175, 75–96.
- Sidle, R.C., Bogaard, T.A., 2016. Dynamic earth system and ecological controls of rainfall-initiated landslides. *Earth-Science Reviews* 159, 275–291.
- Sidle, R.C., Burt, T.B., 2009. Temperate forests and rangelands, in: Slaymaker O, Spencer T, Embleton-Hamann C, (Eds.) *Geomorphology and Global Environmental Change*, Chapter 12. Cambridge University Press, UK, pp. 321–343.
- Sidle, R.C., Ghestem, M., Stokes, A., 2014. Epic landslide erosion from mountain roads in Yunnan, China – challenges for sustainable development. *Natural Hazards and Earth System Science* 14 (11), 3093–3104.
- Sidle, R.C., Noguchi, S., Tsuboyama, Y., Laursen, K., 2001. A conceptual model of preferential flow systems in forested hillslopes: evidence of self-organization. *Hydrol. Process.* 15 (10), 1675–1692.
- Sidle, R.C., Ochiai, H., 2006. *Landslides: processes, prediction, and land use*, Water resources monograph. American Geophysical Union, Washington, DC.
- Sidle, R.C., Ziegler, A.D., Negishi, J.N., Nik, A.R., Siew, R., Turkelboom, F., 2006. Erosion processes in steep terrain-Truths, myths, and uncertainties related to forest management in Southeast Asia. *Forest Ecology and Management* 224 (1–2), 199–225.
- Soil Science Division Staff, 2017. Examination and Description of Soil Profiles, *in: Soil Survey Manual*. C. Ditzler, K. Scheffe, and H.C. Monger (eds.). USDA Handbook 18, Government Printing Office, Washington, D.C., pp. 83–268.
- Soil Survey Staff, 2014. Keys to soil taxonomy (No. 12). Natural Resources Conservation Service, United States Department of Agriculture, Washington, D.C.
- Stokes, A., Atger, C., Bengough, A.G., Fourcaud, T., Sidle, R.C., 2009. Desirable plant root traits for protecting natural and engineered slopes against landslides. *Plant and Soil* 324 (1–2), 1–30.
- Stokes, A., Raymond, P., Polster, D., Mitchell, S.M., 2013. Engineering the ecological mitigation of hillslope stability research into the scientific literature. *Ecological Engineering* 61 (part C), 615–620.
- Stokes, A., Sotir, R., Chen, W., Ghestem, M., 2010. Soil bio- and eco-engineering in China: past experience and future priorities. *Ecological Engineering* 36 (3), 247–257.
- Sun, D., Yang, H., Guan, D., Yang, M., Wu, J., Yuan, F., Jin, C., Wang, A., Zhang, Y., 2018. The effects of land use change on soil infiltration capacity in China: A meta-analysis. *Science of The Total Environment* 626, 1394–1401.
- Tsuboyama, Y., Sidle, R.C., Noguchi, S., Hosoda, I., 1994. Flow and solute transport through the soil matrix and macropores of a hillslope segment. *Water Resour. Res.* 30 (4), 879–890.
- Tsukamoto, Y., Ohta, T., 1988. Runoff process on a steep forested slope. *Journal of Hydrology, Hydrologic Research: The U.S. — Japan Experience* 102, 165–178.
- van Dijk, A.I.J.M., 2002. *Water and Sediment Dynamics in Bench-terraced Agricultural Steeplands in West Java, Indonesia*. Free University, Amsterdam.
- van Schaik, N.L.M.B., 2009. Spatial variability of infiltration patterns related to site

- characteristics in a semi-arid watershed. *CATENA* 78 (1), 36–47.
- Vogel, H.-J., Cousin, I., Ippisch, O., Bastian, P., 2006. The dominant role of structure for solute transport in soil: experimental evidence and modelling of structure and transport in a field experiment. *Hydrology and Earth System Sciences Discussions* 10 (4), 495–506.
- Wang, W.F., Qiu, D.Y., Wu, J.C., Wu, H.M., 1996. *The soils of Yunnan*. Yunnan Science and Technology Press, Kunming.
- Weiler, M., Naef, F., 2003. An experimental tracer study of the role of macropores in infiltration in grassland soils. *Hydrol. Process.* 17 (2), 477–493.
- Wu, G.-L., Liu, Y., Yang, Z., Cui, Z., Deng, L., Chang, X.-F., Shi, Z.-H., 2017. Root channels to indicate the increase in soil matrix water infiltration capacity of arid reclaimed mine soils. *Journal of Hydrology* 546, 133–139.
- Xiao, H.F., Tian, Y.H., Zhou, H.P., Ai, X.S., Yang, X.D., Schaefer, D.A., 2014. Intensive rubber cultivation degrades soil nematode communities in Xishuangbanna, southwest China. *Soil Biology and Biochemistry* 76, 161–169.
- Xu, J., Tao, R., Xu, Z., Bennett, M.T., 2010. China's Sloping Land Conversion Program: Does Expansion Equal Success? *Land Economics* 86 (2), 219–244.
- Capowiez Y., Samartino S., Cadoux S., Bouchant P., Richard G., Boizard H., 2012. Role of earthworms in regenerating soil structure after compaction in reduced tillage systems. *Soil Biology and Biochemistry* 55, 93–103
- Zhang, J., Lei, T., Qu, L., Chen, P., Gao, X., Chen, C., Yuan, L., Zhang, M., Su, G., 2017. Method to measure soil matrix infiltration in forest soil. *Journal of Hydrology* 552, 241–248.
- Zhang, J., Xu, Z., 2016. Dye tracer infiltration technique to investigate macropore flow paths in Maka Mountain, Yunnan Province, China. *J. Cent. South Univ.* 23 (8), 2101–2109.
- Ziegler, A.D., Fox, J.M., Xu, J., 2009. The Rubber Juggernaut. *Science* 324 (5930), 1024–1025.
- Zhu, X., Liu, W., Jiang, X.J., Wang, P., Li, W., 2018. Effects of land-use changes on runoff and sediment yield: Implications for soil conservation and forest management in Xishuangbanna, Southwest China. *Land Degradation & Development* 29, 2962–2974.

Figures & tables

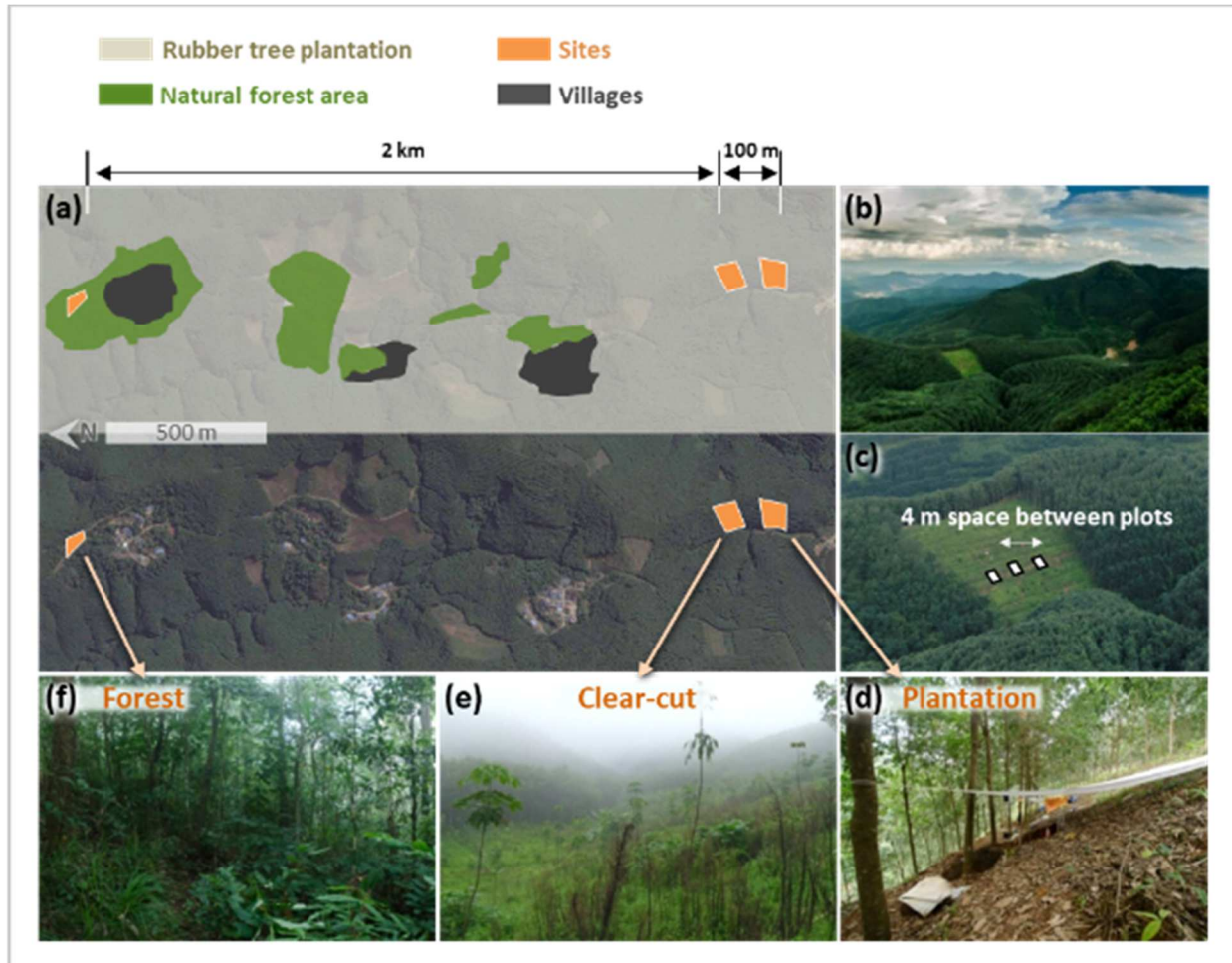


Figure 1

(a) Forest cover and location of field sites in Nan Lin Shan mountain, Yunnan province (China) (Map data: Google, Image ©2015 Digital Globe), (b) general view of the landscape showing the dominance of rubber tree (*Hevea brasiliensis*) plantations and the clear cut site, (c) detail of the location of *in situ* plots mid-slope in the clear-cut site, (d) rubber tree plantation with bare soil interspersed with litter, (e) clear-cut with understorey grass and (f) mixed secondary forest with different understorey strata and litter.

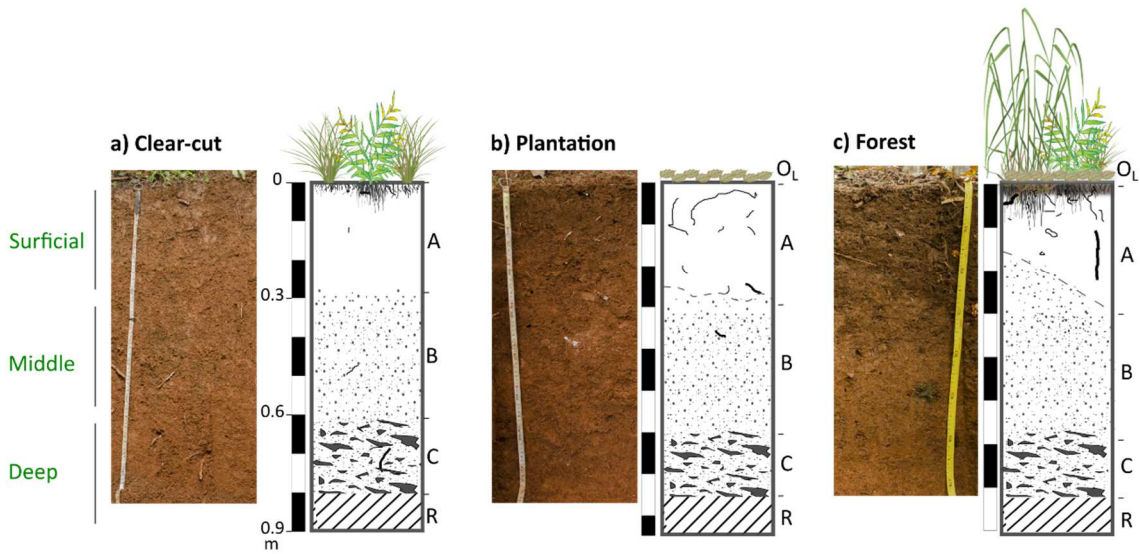


Figure 2

Typical soil profiles (photograph and schematic drawing) for (a) clear-cut, (b) plantation and (c) forest sites. Soil profiles are described in the Materials and Methods section and in Table 2.

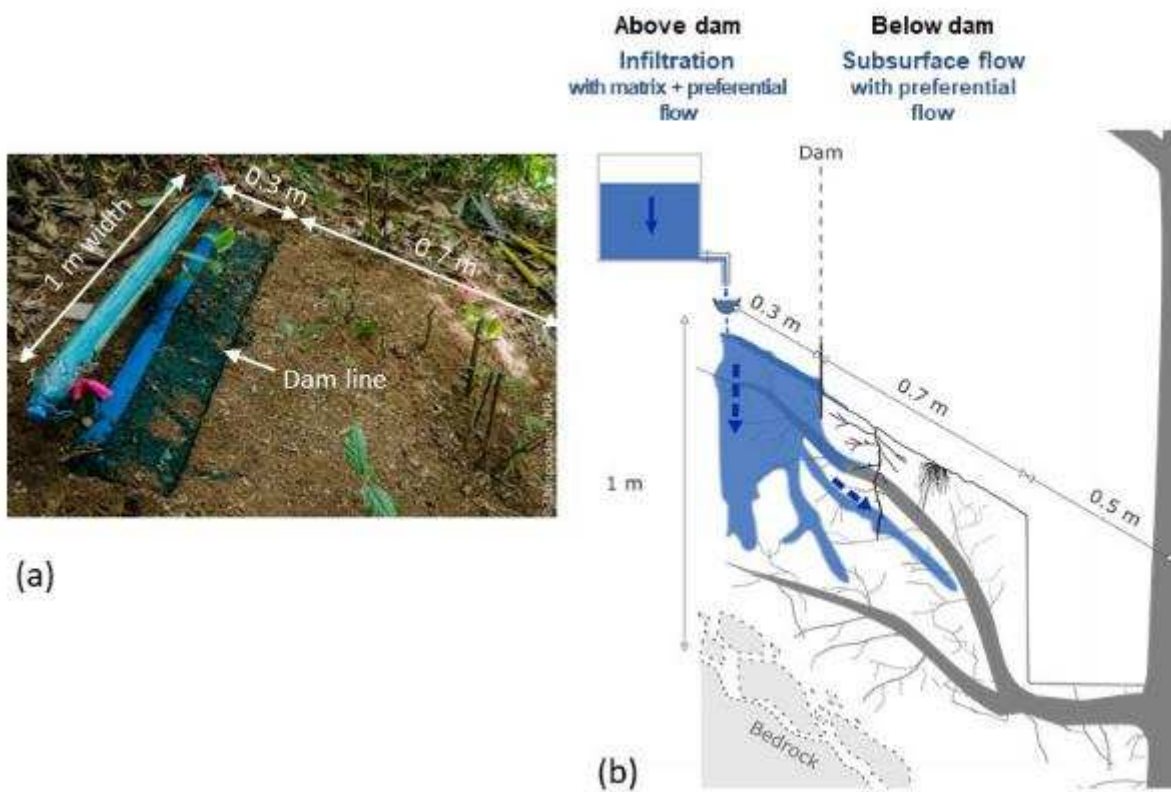


Figure 3

Brilliant blue FCF dyed water was applied onto the soil surface at a distance of 1.5 m above the tree stem. (a) Infiltration was performed using a 1 m long pipe with 30 holes (2 mm diameter). Dyed water was applied at a rate of 10 ml s^{-1} . (b) A metal sheet was installed into soil 0.3 m downslope of the pipe to serve as a dam, to avoid excess runoff and promote infiltration. Hydrological processes differed above and below the dam, with a vertical infiltration with matrix flow and preferential flow above the dam and subsurface flow with preferential flow below the dam.

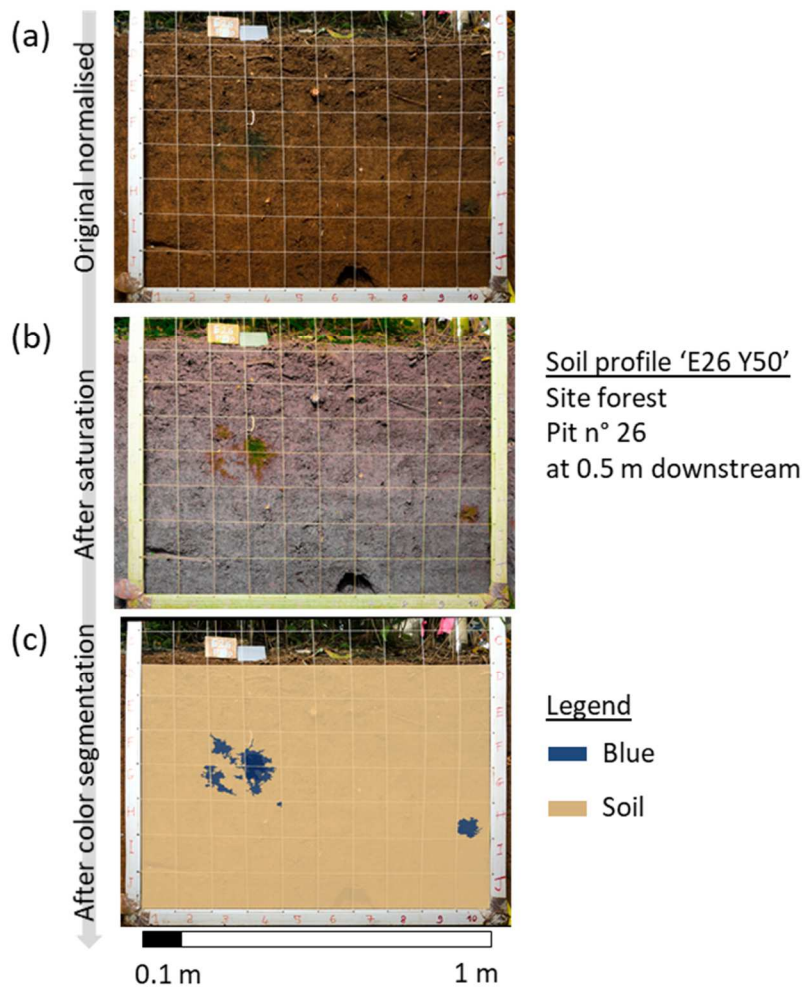


Figure 4

Image analysis procedure. (a) Soil profile photo recalibrated for colours and luminosity. (b) Soil profile photo normalized after colour saturation. (c) Soil profile image after colour segmentation: colour classes were selected using colour threshold 'object classification.' The blue colour refers to areas stained with brilliant blue FCF dyed water.

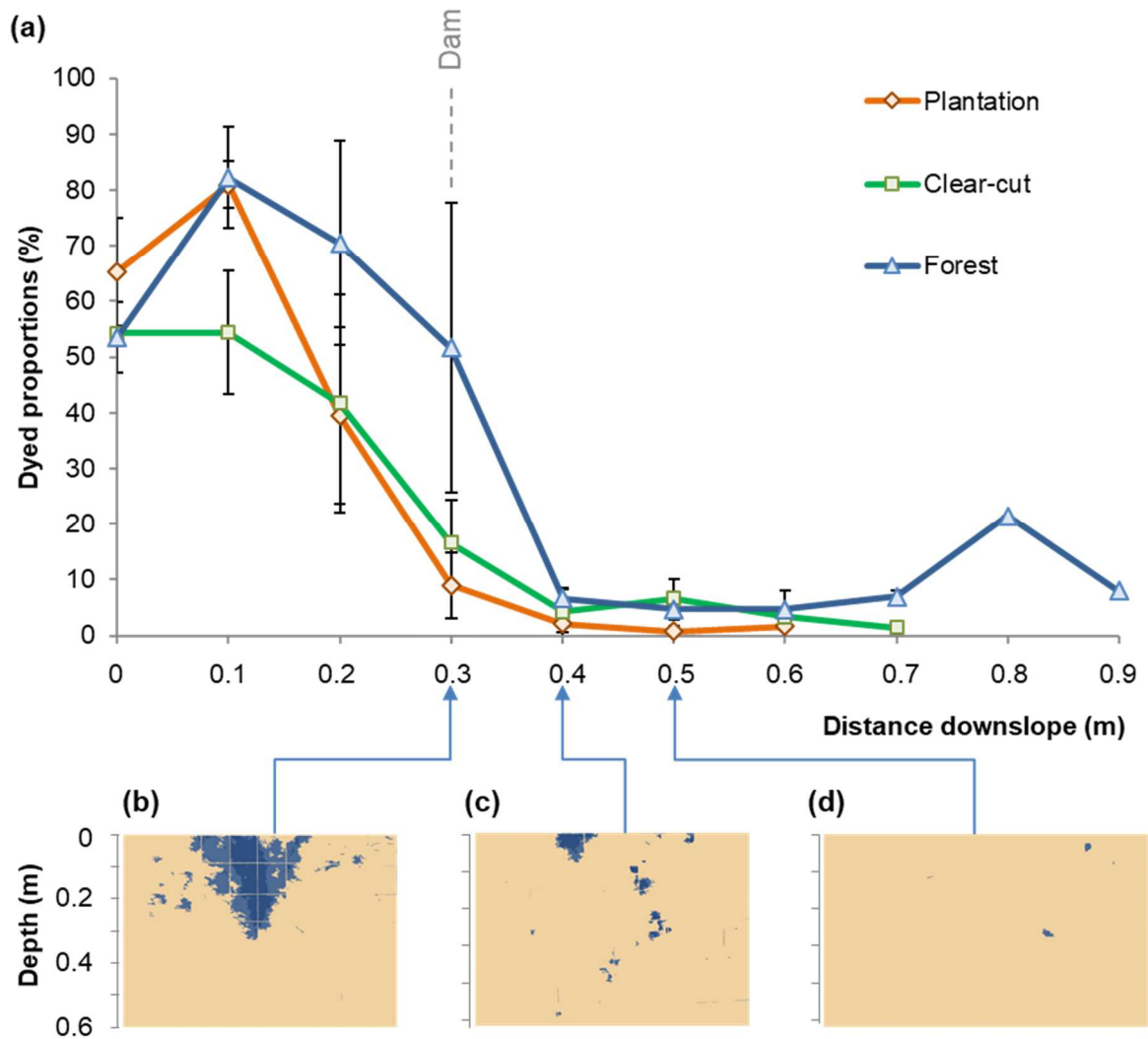


Figure 5

(a) Mean proportion of surface area with Brilliant Blue FCF dyed water flowing downslope along the plot for each site (distance along the slope from the point where dye was applied (0.0 m) and at each subsequent profile every 0.1 m downslope). Data are mean \pm standard error. Example of three soil profiles at the plantation site at (b) 0.3 m, (c) 0.4 m and (d) 0.5 m downslope.

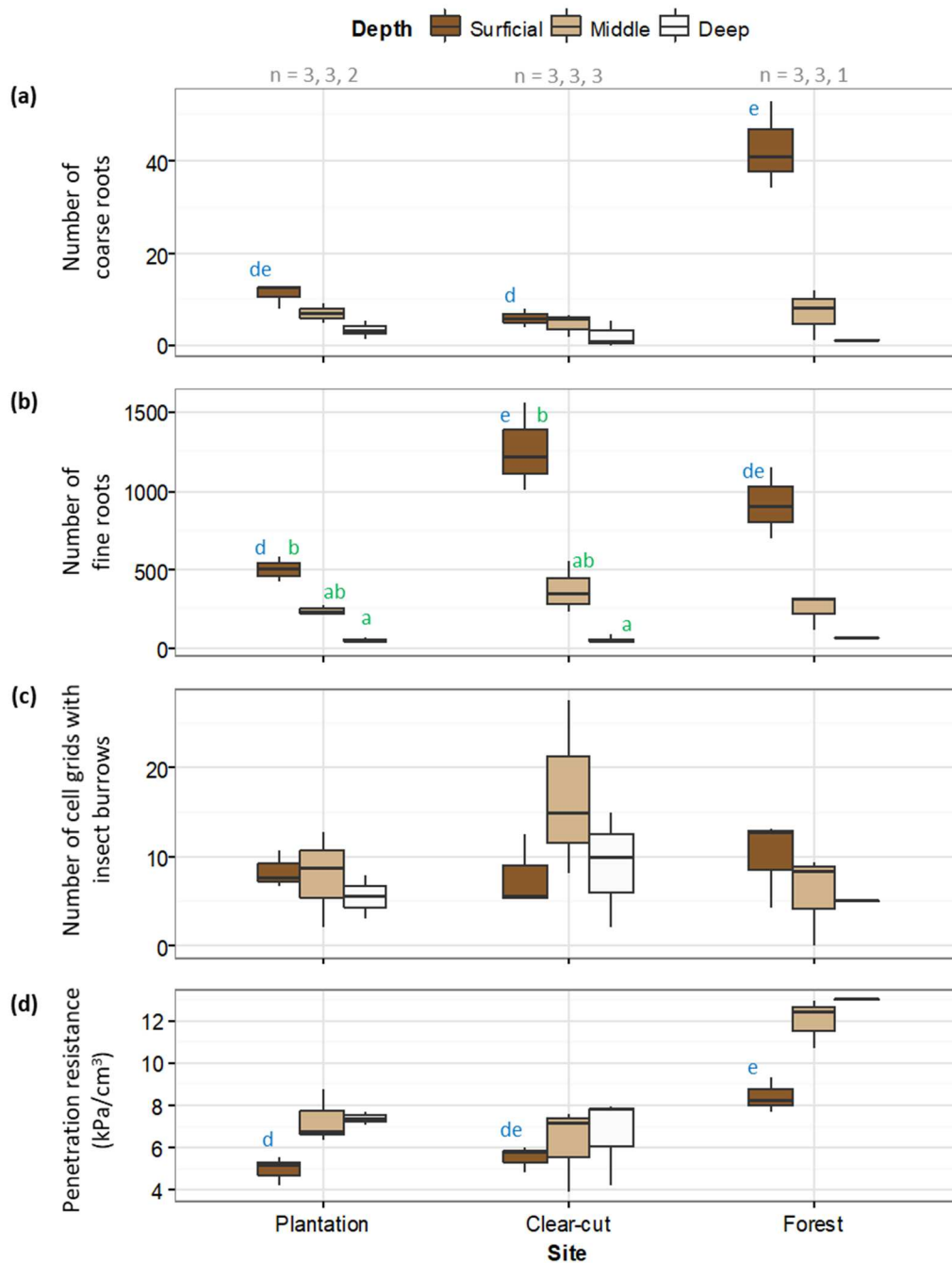


Figure 6

Soil depth relationships with (a) mean number of coarse roots per horizon per soil profile, (b) mean number of fine roots per horizon soil profile, (c) mean number of cell grids with insect burrows per horizon soil profile and (d) resistance to penetration per horizon soil profile. Data are significantly different ($P < 0.05$) when letters above the boxplots differ. Letters 'a' and 'b' correspond to tests with depth as the factor and letters 'd' and 'e' correspond to tests with site as the factor. The Kruskal-Wallis rank sum test chi-square is the coefficient of determination at the probability level.

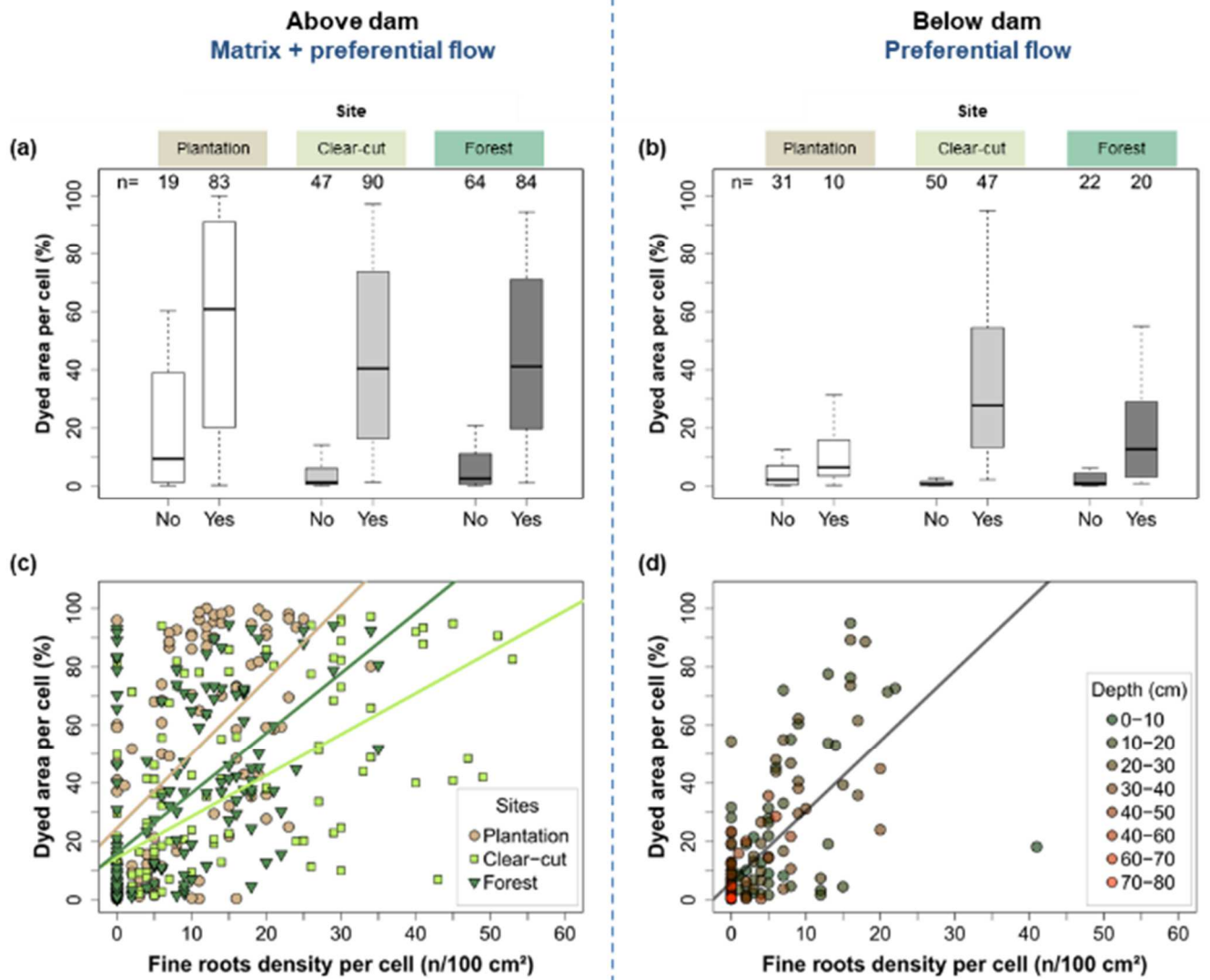


Figure 7

Relationships between the surface area of blue dye and fine roots. Boxplot comparing the blue dye distribution in terms of fine root absence (No) or presence (Yes) at a) above the dam and b) below the dam. Scatterplot showing dyed area in relation to c) the number of fine roots, with site highlighted with different colours above the dam in which trends are $y_{\text{plantation}} = 2.55x + 24.50$, $P < 0.001$, $R^2 = 0.29$, $y_{\text{clear-cut}} = 1.41x + 14.40$, $P < 0.001$, $R^2 = 0.41$, $y_{\text{forest}} = 2.06x + 15.95$, $P < 0.001$, $R^2 = 0.33$ and (d) below the dam with depth highlighted with different colours in which the general trend is $y = 2.42x + 6.02$, $P < 0.001$, $R^2 = 0.46$. Trends are obtained from linear models between %dyed surface area and the number of fine roots.

Strata	Species	Family	Mean abundance cover (%)		
			Plantation	Clear-cut	Forest
Grass	<i>Ageratum sp.</i>	Asteraceae			2
	<i>Bambusoideae sp.</i>	Poaceae		30	30
	<i>Crotalaria sp.</i>	Fabaceae		2	2
	<i>Cyclosorus aridus</i>	Thelypteridaceae		13	13
	<i>Cyperus sp.</i>	Cyperaceae		2	2
	<i>Dianella ensifolia</i>	Asphodelaceae		2	2
	<i>Ficus sp.</i>	Moraceae		2	2
	<i>Hedyotis sp.</i>	Rubiaceae		42	
	<i>Hedyotis sp. 2</i>	Rubiaceae		2	2
	<i>Homalanthus sp.</i>	Euphorbiaceae		2	2
	<i>Melastoma sp.</i>	Melastomataceae		2	2
	<i>Microstegium ciliatum</i>	Poaceae		2	2
	<i>Phyllanthus sp.</i>	Phyllanthaceae		10	10
	<i>Pteridium revolutum</i>	Pteridiaceae		2	2
	<i>Rhus chinensis</i>	Anacardiaceae		2	2
	<i>Scleria ciliaris</i>	Cyperaceae		2	2
	<i>Setaria</i>	Poaceae		2	2
	<i>Setaria palmifolium</i>	Poaceae		10	10
<i>Thysanolaena maxima</i>	Poaceae			2	
<i>Urena lobata</i>	Malvaceae		4	4	
Liana	<i>Lygodium flexuosum</i>	Lygodiaceae		2	2
Shrub	<i>Dalbergia</i>	Fabaceae			2
	<i>Scleria ciliaris</i>	Cyperaceae			2
	<i>Smilax hypoglauca</i>	Smilacaceae			2
Tree	<i>Anthocephalus chinensis</i>	Rubiaceae			11
	<i>Aporosa yunnanensis</i>	Phyllanthaceae			6
	<i>Archidendron monadelphum</i>	Fabaceae, Mimosoideae			6
	<i>Castanopsis mekongensis</i>	Fagaceae			6
	<i>Grewia acuminata</i>	Malvaceae			11
	<i>Hevea brasiliensis</i>	Euphorbiaceae	100	100	
	<i>Syzygium cumini</i>	Myrtaceae			6

Table 1 - Plant species present at different sites

Plant species are divided into groups depending on vegetation strata. Tree species present on experimental plots are highlighted in bold. The species names noted sp. and sp2 were identified to the genus level only.

Site	Horizon	Depth (m)	Particle size distribution (%)			Texture	Organic matter OM (%)	pH _{water}	Density (mean±SD)	Color (Munsell chart)	Color
			Sand (2 mm - 50 µm)	Silt (50 µm - 2 µm)	Clay (< 2 µm)						
<i>Plantation</i>	<i>Surficial - A</i>	0 - 0.3	24.8	31.9	43.3	Clay	3.45	5.28	0.92 ± 0.07	10 YR 4/6	dark yellowish brown
	<i>Middle - B</i>	0.3 - 0.6	23.7	32.3	44.0	Clay	2.76	5.18	1.09 ± 0.09	7.5 YR 5/8	strong brown
	<i>Deep - C</i>	0.6 - 0.8	27.5	30.7	41.8	Clay	1.69	5.31	NA	7.5 YR 6/8	reddish yellow
<i>Clear-cut</i>	<i>Surficial - A</i>	0 - 0.3	22.3	31.7	46.0	Clay	4.98	4.66	1.01 ± 0.08	10 YR 4/6	dark yellowish brown
	<i>Middle - B</i>	0.3 - 0.6	20.0	39.1	40.9	Clay	2.09	4.70	1.09 ± 0.11	7.5 YR 5/8	strong brown
	<i>Deep - C</i>	0.6 - 0.8	24.0	39.8	36.2	Clay loam	1.45	4.48	NA	7.5 YR 6/8	reddish yellow
<i>Forest</i>	<i>Surficial - A</i>	0 - 0.3	27.3	26.1	46.6	Clay	5.26	4.41	1.06 ± 0.1	10 YR 4/6	dark yellowish brown
	<i>Middle - B</i>	0.3 - 0.6	28.0	25.8	46.2	Clay	3.28	4.35	1.22 ± 0.09	7.5 YR 5/8	strong brown
	<i>Deep - C</i>	0.6 - 0.8	22.8	25.5	51.7	Clay	1.88	4.61	NA	7.5 YR 6/8	reddish yellow

Table 2 - Soil properties of field sites in Nan Lin Shan mountain

Textural classification was performed following the USDA soil taxonomy.

a) Above dam (Y < 0.3 m)

Groups	Estimate	Std. err.	df	t	P
(Intercept)	17.01	2.82	15.13	6.03	< 0.001
Fine roots : Site Plantation	2.77	0.29	102.70	9.52	< 0.001
Fine roots : Site Forest	2.08	0.24	256.71	8.72	< 0.001
Fine roots : Site Clear-cut	1.31	0.16	223.17	8.36	< 0.001

b) Below dam (Y > 0.3 m)

Groups	Estimate	Std. err.	df	t	P
(Intercept)	9.54	3.28	72.85	2.91	< 0.01
Fine roots	0.99	0.40	173.25	2.47	< 0.05
Depth	-0.15	0.07	178.76	2.10	< 0.05
Fine roots : Depth	0.05	0.02	177.63	3.02	< 0.01

Table 3

Estimated parameters for fixed and random effects of selected LMEr explaining the variation of surface area of soil stained with Brilliant Blue FCF dyed water at the microscale: (a) above the dam and (b) below the dam. Estimates are the parameter estimates with σ standing for standard deviation for random effects. Std. Err are the standard errors of the estimates. t represents the ratio of estimates and their standard errors, and P is the associated probability value from a t distribution.

Declaration of interest

The authors declare that they have no competing interests